Received 3 June 2024, accepted 17 August 2024, date of publication 26 August 2024, date of current version 5 September 2024.

Digital Object Identifier 10.1109/ACCESS.2024.3449444

RESEARCH ARTICLE

A New Parametric Three Stage Weighted Least Squares Algorithm for TDoA-Based Localization

IGOR KRAVETS[1,2], OLEG KAPSHII[2,3], OSTAP SHUPARSKYY[4], AND ANDRIY LUCHECHKO[1,2]

[1]Department of Sensor and Semiconductor Electronics, Ivan Franko National University of Lviv, 79000 Lviv, Ukraine
[2]Infineon Technologies AG, 79000 Lviv, Ukraine
[3]Department of Information Systems and Computer Modelling, Ukrainian National Forestry University, 79057 Lviv, Ukraine
[4]Faculty of Electronics and Computer Technologies, Ivan Franko National University of Lviv, 79000 Lviv, Ukraine

Corresponding author: Oleg Kapshii (Oleg.Kapshii@infineon.com)

ABSTRACT The time-difference-of-arrival method is popular for indoor tracking systems due to its simple usage, efficiency, performance, and power economy. To solve the non-linear optimization problem of tag coordinates calculation from number of measurements on synchronized anchors, often a low complexity linear least square technique or one of its more advanced variants are used: e.g. two-step weighted least squares or constrained weighted least squares methods. However, these techniques suffer from an ill-conditioned problem for a specific anchors and tags locations, so a new Parametric Three-stage Weighted Least Squares algorithm is proposed. New algorithm identifies a family of solutions and works even in rank deficient conditions, ensuring accurate and reliable estimates for core areas of the anchor nodes mesh cells. To achieve the best performance outside the core area, the hybrid algorithms are also introduced utilizing the eigenvalue ratio and independent parameter correlation criteria to switch between algorithms. The performance of the proposed algorithms was analyzed for Gaussian noise, reference and non-reference anchors desynchronization errors, and multipath shadowing environment for square, hexagon, and triangular anchor node mesh patterns.

INDEX TERMS TDoA localization, linear least square, 2WLS, P3WLS, ill-conditioned problem.

I. INTRODUCTION

Things localization is still an active and popular topic in the research domain despite having GPS available worldwide and using it in airplanes, agriculture, phones, watches, and other smart things. The problem with GPS is that it does not work indoor, it has limited accuracy in standard mode, and it requires comparably a lot of energy to determine position. There are still many use-cases available that need something simpler, cheaper, and more efficient, that works in limited area of a room, building, warehouse, or car e.g. Over the past decade, several localization technologies have been developed utilizing popular ISM radio band: WiFi-, BLE-, Radar- based solutions. Usually, these solutions measure signal strength, signal delay and/or channel transfer function converting them into the distance and direction of arrival estimates later used for location calculation based on triangulation, trilateration, or fingerprinting (mapping signal patterns in considered areas) techniques [21].

With deploying UWB tags by Apple [25] and later by Samsung, intensification of work on UWB standardization [22] and speeding up BLE channel sounding (CS) technology [23], [24] development, the simplicity and effectiveness of indoor localization techniques noticeably improved while number of requests and application ideas rapidly increased. Since UWB distance measurement devices already present on the market, many solutions stop their choice on this technology. But major question remains – how to build the system and which methods should be used for the optimal functioning and for the lower cost.

The associate editor coordinating the review of this manuscript and approving it for publication was Haibin Sun.

To determine location of a tag or device in a large open space area, usually a number of anchors with known positions are used. In such a system, the relative position of the tag should be calculated and the commonly used approach in a set of practical use-cases is the Time Difference of Arrival (TDoA). It is a very popular and efficient technique for devices localization when there is a large network of anchors available. The anchors themselves in the system must be synchronized, but tags/devices should not. The functionally, in this case is limited to tags unique packet broadcasting when tag location is required. The anchors in the system register the time of the packet arrival, the system determines time difference in relation to a reference anchor and calculates the tag position using this information.

TDoA brings several advantages for location systems:

- Tags do not communicate with each anchor individually. In comparison to the two-way ranging (TWR), where a tag must establish separate messages exchange with each available anchor, in the TDoA scenario only one locationing message should be transmitted by a tag to locate its position by a system. This leads to significant decrease of number of communication events and increase the tag's battery life.
- Also, because tags do not need to know the available anchors, their configurations, positions, addressing as for the case of the TWR system, the number of anchors operating in the system are fully scalable. Adding more anchors does not require any reconfiguration of the tags. All changes are made in a real-time locating system (RTLS) server, which just provide the tag position to a requestor.
- Tags use only short portion of time to send a locationing message, therefore higher number of tags can work in the vicinity simultaneously, significantly exceeding possibilities of TWR-based approaches.

In some way, the location calculation for a TDoA system is similar to trilateration [5], where the system estimates tag's location based on circles intersection, but rather with hyperbolic curves intersection [6]. Solution of this task is not mathematically trivial as the locationing problem deals with a nonlinear function of tag coordinates and is considered as a non-convex optimization problem. The solutions based on Maximum Likelihood iterative Gauss-Newton, Steepest Descent, and Levenberg-Marquardt algorithms are computationally complex and not always converge [7]. The conventional method of linearization based on Taylor series decomposition [5], [9], [27] does not guarantee convergence and a step of initial guessing is required which accuracy influences the performance.

Neural network-based approaches [12] can also tackle this problem showing good results, but solution is fixed to unique anchors nodes mesh configuration and changes in the system are not allowed. If any anchor position is changed, the neural network should be completely retrained. The similar technology used in [13] for multi-static system. The NN often proposed to use in UWB TDoA systems for a determined position refining, but the methods need usually channel impulse response measuring [14], [15]. Often tracking with IMU sensors [16] or signal mapping/fingerprinting [17] is applied.

There are several approaches that use geometrical properties analysis where relations between hyperbolic lines and their intersection points [18] are considered. The circle shrinking method is based on iterative founding of distance circle radiuses with intersection area in range of a specified threshold [2], [19]. This method can be quite computationally intensive [20]. Large number of computations also can require iterative approaches like semidefinite programming methods [28].

In very popular and low complexity linear least squares (LLS) based methods [5], [8], [28], the system is linearized by adding an additional variable with breaking a relationship between it and a tag position. This allows to solve linear systems but increases error level. More advanced variants: two-step weighted least squares (2WLS) [1], [6] and constrained weighted least squares (CWLS) [10] techniques try to return in calculation the relations between the variables. However, a matrix ill-conditioned problem [2], [3] occurs for some tag location and specific anchors configurations. The Separated CWLS method instead of eliminating the additional variable proposes an algorithm of estimation it from a quadratic equation [3]. But it is not always successful in determination of a global optimal solution.

The matrix ill-conditioned problem in WLS-based methods can be considered as negligible one, because the anchors geometric configuration can be easily modified to break the symmetry in most of the cases. But the ill-conditioned problems can appear also for non-symmetric systems when noise or NLoS conditions are present and distort the measurements in a specific way. Considering that the WLS-based methods are easy to implement and widely used, the question of dealing with the problem is still actual. This paper proposes a new Parametric Three-stage Weighted Least Squares (P3WLS) algorithm, which extends the ill-conditioned problem solving with some geometrical analysis of a system and shows a way how to determine a solution in such case.

The rest of the paper is organized in the following way. The second section includes basics of TDoA methods and analysis of widely-used least squares calculation approach. The third and fourth sections describe the proposed new three-stage least squares algorithm. Sections V-VII provide information about algorithms performance investigation under different variations and configurations. The last section presents conclusions, and future prospects.

II. TIME-DIFFERENCE-OF-ARRIVAL

A lot of ultrawide-band indoor tracking systems use the Time-Difference-Of-Arrival principle based on measuring times when a packet from a tag (Tx) is received by anchors Rx_i, $i = 2..N$, N – number of anchors (Fig. 1). Since receivers are mutually synchronized, it is possible to capture a specific moment when transmitter/source tag signal reaches the specific receiver t_i and the relative time delays $\tau_{i1} = t_i - t_1$ can be calculated between the signal arrival at time t_1 at reference receiver located in the axis origin ($x_1 = 0, y_1 = 0$) and the signal arrival at other anchors in known locations (x_i, y_i).

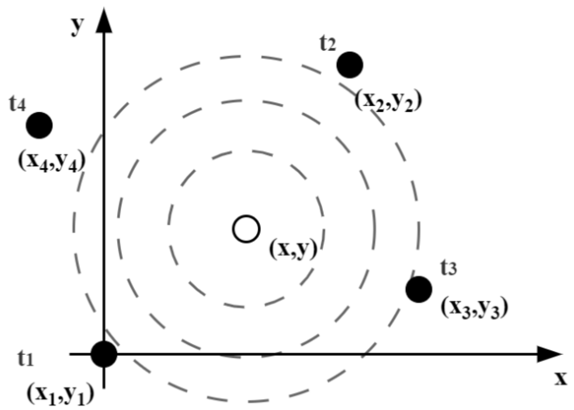

FIGURE 1. Example of TDOA location setup.

For convenience, let's express relative distance between transmitter and receiver as:

$$d_i = \|\mathrm{Rx}_i - \mathrm{Tx}\|, \tag{1}$$

where $\mathrm{Rx}_i = \begin{bmatrix} x_i \\ y_i \end{bmatrix}$ and $\mathrm{Tx} = \begin{bmatrix} x \\ y \end{bmatrix}$. Note, the first relative distance $d_1 = \|\mathrm{Rx}_1 - \mathrm{Tx}\| = \|\mathrm{Tx}\| = d$, where $d = \sqrt{x^2 + y^2}$. The TDoA system of equations is this case will be defined as:

$$c\tau_{i1} = d_i - d_1 = d_i - d = \|\mathrm{Rx}_i - \mathrm{Tx}\| - \|\mathrm{Tx}\|, \tag{2}$$

where c – speed of signal propagation. This system of equations is a nonlinear one. Thus, locating the source is not a trivial task because the TDOA measurements are nonlinear functions of the source coordinates.

A. LINEAR LEAST SQUARES ALGORITHM

To avoid non-linearities the Linear least squares approach has been proposed. It takes advantages of the linear operation via the introduction of an additional variable. Without considering the known relationship of this variable with the source position, it is estimated together with the source position by solving a system of linear equations. One version of such algorithm, namely, two-step weighted least squares [6] is the most interesting solutions of TDoA nonlinear system of equations. It was investigated extensively by NASA Johnson Space Center for lunar / Mars rover proximity tracking applications and is simple and efficient enough to be reused for indoor positioning [1]. The 2WLS method idea is to return back in the computation the ignored relations between variables at the second stage of the algorithm. The whole flow is shown below.

By taking d as an independent variable, the LLS method creates a linear set of equations for the $[x, y, d]$ variables:

$$2xx_i + 2yy_i + 2dc\tau_{i1} = x_i^2 + y_i^2 - (c\tau_{i1})^2 \tag{3}$$

In this way (3) can be expressed in a matrix form:

$$G_1 p_1 \approx h_1, \tag{4}$$

where:

$$G_1 = 2\begin{bmatrix} x_2 & y_2 & c\tau_{21} \\ x_3 & y_3 & c\tau_{31} \\ \vdots & \vdots & \vdots \\ x_N & y_N & c\tau_{N1} \end{bmatrix}, h_1 = \begin{bmatrix} x_2^2 + y_2^2 - (c\tau_{21})^2 \\ x_3^2 + y_3^2 - (c\tau_{31})^2 \\ \vdots \\ x_N^2 + y_N^2 - (c\tau_{N1})^2 \end{bmatrix},$$

$$p_1 = \begin{bmatrix} x \\ y \\ d \end{bmatrix}.$$

The minimal number of anchors we need for the system to be solved in 2D case equals to four. In this case the system has only one solution and can be evaluated in the following way:

$$\hat{p}_1 = G_1^{-1} \cdot h_1 \tag{5}$$

However, in a case of $N > 4$, the system is overdetermined and has no unique solution. Correspondingly, the optimal solution should be defined by additional constrains (e.g. Lagrange multipliers).

The 2WLS method [1] is used to solve overdetermined system of linear equations. In the first stage we search $\hat{p}_1$ (source location and additional variable) which minimizes least squares error $\varepsilon_1 = \mathrm{h}_1 - \mathrm{G}_1 p_1$ variance:

$$\hat{p}_1 = arg \min_{p_1} \varepsilon_1^{\mathrm{H}} \varepsilon_1. \tag{6}$$

To make solution more precise weighted error $\varepsilon_1^H W_1 \varepsilon_1$ is recommended. Weighting factor in this case W_1 can be chosen in the form:

$$W_1 = \frac{1}{4c^2} B_1^{-1} Q^{-1} B_1^{-1}, \tag{7}$$

where TDOA measurements error is assumed to be a Gaussian random vector with covariance matrix Q such that

$$\tau \in \eta(0, Q), \tag{8}$$

and

$$B_1 = I\begin{bmatrix} d_2 \\ d_3 \\ \vdots \\ d_N \end{bmatrix}. \tag{9}$$

Least squares weighted solution estimate for given conditions is equal to:

$$\hat{p}_1 = \left(G_1^H W_1 G_1\right)^{-1} G_1^H W_1 h_1. \tag{10}$$

Stage II of the 2WLS method exploits the relationship between the additional variable d and the source position. So, in order to satisfy the $d^2 = x^2 + y^2$ relationship, the following equation must hold:

$$G_2 p_2 \approx h_2, \tag{11}$$

where

$$G_2 = \begin{bmatrix} 1 & 0 \\ 0 & 1 \\ 1 & 1 \end{bmatrix}, p_2 = \begin{bmatrix} x^2 \\ y^2 \end{bmatrix}, h_2 = \hat{p}_1^2.$$

Least squares method is used to solve linear system of equations (11) by minimizing the estimation error $\varepsilon_2 = h_2 - G_2 p_2$ variance. To make solution more precise, a weighting factor W_2 might be used. In this case we minimize the weighted noise $\varepsilon_2^H W_2 \varepsilon_2$, with:

$$W_2 = \frac{1}{4} B_2^{-1} G_1^H W_1 G_1 B_2^{-1}, \tag{12}$$

where $B_2 = I p_1$.

B. MATRIX ILL-CONDITIONED PROBLEM

In general, 2WLS method provides estimation performance close to Cramér–Rao lower bound at sufficiently small noise conditions with relatively small resources requirement [1]. However, a matrix ill-conditioned problem occurs when the distances from the tag to some receivers are identical, approximately the same, or source is located on some of the lines of symmetry. The error for such conditions increases significantly. For example (Fig. 2), when the tag is located at or near the centroid of the receivers whose geometry is close or equal to a uniform circular array, the 2WLS performs poorly. The reason is the system matrix which defines a solution of the linear equations ($G_1^H \cdot G_1$) is singular or ill-conditioned. The similar situation is for the case of four anchors located in the middle of each wall in the rectangular room or four anchors in four corners of a square room (Fig. 2). The ill-conditioned problem occurs when source is located on two hyperbolic curves for the first case and on the two lines of symmetry for the second.

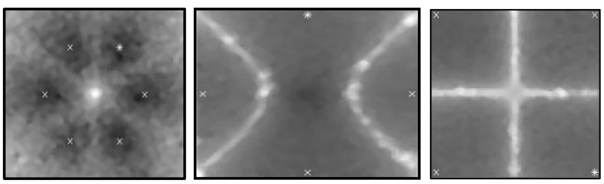

FIGURE 2. Examples of 2LS matrix ill conditioned problem locations. Lighter color mark places where 2LS calculated position will have large systematic error. Small crosses mark anchors positions, star – a reference anchor.

Matrix ill-conditioned problem appears in specific locations when there is no dependency between one or more tag location coordinates and the independent variable. In such a case the solution might be simplified as the matrix ($G_1^H \cdot G_1$) rank is smaller than the matrix size. But the level and an approach of simplification is difficult to evaluate because there might be only one coordinate independent on the distance, two, or three (if 3D space is considered). Someone may test dependencies and simplify system of equations accordingly but taking into account the time estimation error, it is nearly impossible to choose proper system simplification as there always will be all tiny (caused by measurement noise) correlations between independent variables. There are several methods to improve 2WLS in case of ill-condition problem happens [3], but in general they try to find a better location estimation during the first stage. Unfortunately, in case of ill-conditioned problem there is no best estimate because there exists a whole family of possible solutions that must be taken into account.

III. PARAMETRIC THREE STAGE WEIGHTED LEAST SQUARES ALGORITHM

The Parametric Three-Stage Weighted Least Squares method is a variation of NASA 2WLS algorithm improved to work in the ill-conditioned configurations. The P3WLS method instead of searching unique solution during the first and second stages works with the whole family of best solutions. The family is described as a function of some parameter α and is used during the third stage to determine the best solution. Fig. 3 shows the basic idea of P3WLS: the first estimate of one of the possible system solutions (point 1), defining the set of solutions for given conditions (line 2), finding the best solution in the set (points 3) as an intersection with a conic surface representing coordinates-distances relations.

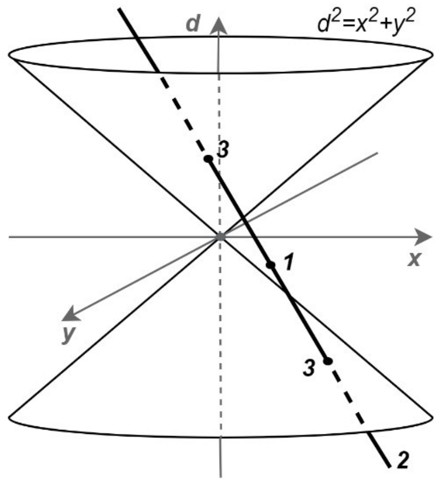

FIGURE 3. P3WLS algorithm stages: point 1 – the initial estimation of one of possible solutions, line 2 – the set of possible solutions, points 3 – the best solutions.

A. THE FIRST STAGE

During the first stage of P3WLS any solution of the linear system (4) is calculated. We can use any of existing methods to obtain the best guess estimate [4], for example, Tikhonov regularization approach [11]. Alternatively, we can set a value of the independent variable to any good prediction. In the Fig. 3, for example, the $d = 0$ value (marked 1) is selected as the first estimate. At this stage the goal is to obtain the estimated value as close to ground truth as possible to minimize errors on the next stages. This can be done in different ways such as using 2WLS methods, average room distance estimate, or by using previous tracking distance estimate.

B. THE SECOND STAGE

During the second stage we estimate a family of solutions which describes given configuration in the best way. Specifically, we search not for the unique solution which minimizes weighted estimation error $\varepsilon_1^H W_1 \varepsilon_1$, but rather for the set of solutions $\hat{p}_1$ which provide the smallest error possible:

$$\begin{aligned}\hat{\varepsilon}_1^H W_1 \hat{\varepsilon}_1 &= \left(h_1 - G_1\hat{p}_1\right)^H W_1 \left(h_1 - G_1\hat{p}_1\right)\\ &< \min_{p_1} < \left(\varepsilon_1^H W_1 \varepsilon_1\right) + \delta,\end{aligned} \tag{13}$$

where δ is a small parameter limiting solutions family dimension.

Lemma: In case of the ill-condition problem, the least squares solutions $\hat{p}_1$ of the TDoA system of linear equations $G_1 p_1 \approx h_1$ forms a line in the direction of the linear span of the $G_1^H W_1 G_1$ matrix eigenvector with a smallest eigenvalue.

Proof: Suppose $\hat{p}_1$ is the weighted least squares solution of a system of linear equations $G_1 p_1 \approx h_1$. In such a way:

$$\hat{p}_1 = \underset{p_1}{argmin}\, \varepsilon_1^H W_1 \varepsilon_1,$$

and the following equality holds:

$$G_1^H W_1 G_1 \hat{p}_1 = G_1^H W_1 h_1.$$

In case of the ill-conditioned problem, the matrix $G_1^H W_1 G_1$ suffers rank deficiency, and there is at least one zero eigenvalue $\lambda_{min} = 0$ with corresponding eigenvector v_{min}. The eigenvalue definition ($G_1^H W_1 G_1 v_{min} = \lambda_{min} v_{min}$) defines the equality $G_1^H W_1 G_1 v_{min} = 0$.

It means, that any other $\hat{p}_1^* = \hat{p}_1 + \alpha \mathrm{v}_{\min}$, $\alpha \in \mathbb{R}$ is also the least squares solution of the linear equations system, because:

$$\begin{aligned}G_1^H W_1 G_1 \hat{p}_1^* &= G_1^H W_1 G_1 \left(\hat{p}_1 + \alpha v_{min}\right)\\ &= G_1^H W_1 G_1 \hat{p}_1 + \alpha G_1^H W_1 G_1 v_{min}\\ &= G_1^H W_1 G_1 \hat{p}_1 = G_1^H W_1 h_1.\end{aligned}$$

End of proof

Note, (Fig. 4), the least squares solutions $\hat{p}_1$ (red dots) are located around the direction of the linear span of the $G_1^H W_1 G_1$ matrix eigenvector also in a case of large stiffness ratio of the system which is a typical case for the TDoA systems. The stiffness ratio of the linear system of equations is defined as the ratio of the largest and smallest eigenvalues of the matrix and is large in case of strong dependencies between linear equations [26].

Let v_{min} be the eigenvector of $G_1^H W_1 G_1$, that corresponds to the smallest eigenvalue $\lambda_{min} = \min\left|\lambda_k\right|$, among all eigenvalues λ_k. The least squares error change is minimal along the direction of v_{min}. So, if $\hat{p}_1$ is the TDoA system solution estimation at the first stage, the family of other solutions $\hat{p}_2$ will be located around the spatial line expressed as:

$$\hat{p}_2 = \hat{p}_1 + \alpha v_{min}, \tag{14}$$

where $v_{min} = \begin{bmatrix} v_x \\ v_y \\ v_d \end{bmatrix}$, $\hat{p}_1 = \begin{bmatrix} \hat{x}^{(1)} \\ \hat{y}^{(1)} \\ \hat{d}^{(1)} \end{bmatrix}$, $\hat{p}_2 = \begin{bmatrix} \hat{x}^{(2)} \\ \hat{y}^{(2)} \\ \hat{d}^{(2)} \end{bmatrix}$, and α is an independent parameter of the parametric line.

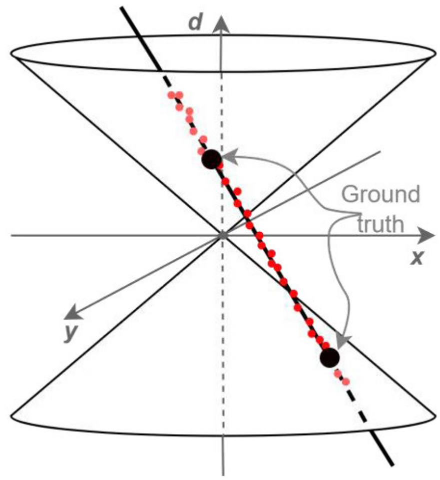

FIGURE 4. Example of the solutions family created due to matrix perturbations or measurement noise.

C. THE THIRD STAGE

During the third stage of the P3WLS algorithm the finest solution estimation of the TDoA system of equations is identified as an intersection of family line $\hat{p}_2$ with the conic surface:

$$d^2 = x^2 + y^2. \tag{15}$$

There can be none, one, two, or infinite number of solutions. But in case of sufficient number of anchors and relatively small measurement noise, there are two solutions which can be determined as roots of the quadratic equation:

$$a\alpha^2 + b\alpha + c = 0, \tag{16}$$

where $a = v_x^2 + v_y^2 - v_d^2$, $b = 2v_x\hat{x}^{(1)} + 2v_y\hat{y}^{(1)} - 2v_d\hat{d}^{(1)}$, and $c = \left(\hat{x}^{(1)}\right)^2 + \left(\hat{y}^{(1)}\right)^2 - \left(\hat{d}^{(1)}\right)^2$. The solution of the quadratic equation provides an estimate of the TDoA fine solutions:

$$\hat{p}_3 = \hat{p}_1 + \alpha_{1,2} v_{min}, \tag{17}$$

where $\alpha_{1,2} = \frac{-b \pm \sqrt{b^2 + 2ac}}{2a}$ and $\hat{p}_3 = \begin{bmatrix} \hat{x}^{(3)} \\ \hat{y}^{(3)} \\ \hat{d}^{(3)} \end{bmatrix}$.

Points $\hat{p}_3$ represent the intersections of the line 2 and the conic surface (Fig. 3). Variety of cases occur in practical configurations, and it is often not easy to certainly determine the right solution. The most common conditions during the data processing are following (shown for four anchors in a square room example in Fig. 5):

1. $\alpha_{1,2}$ are real solutions and the family line intersects both positive and negative branches of the cone. The correct solution is the one with $\hat{d}^{(3)} > 0$.
2. $\alpha_{1,2}$ are real and equal. There is a one solution only. In case of noisy data $\alpha_{1,2}$ might be complex numbers. It means the line does not intersect any branch of the cone. In such a case it is recommended to locate the closest cone points to the family line.

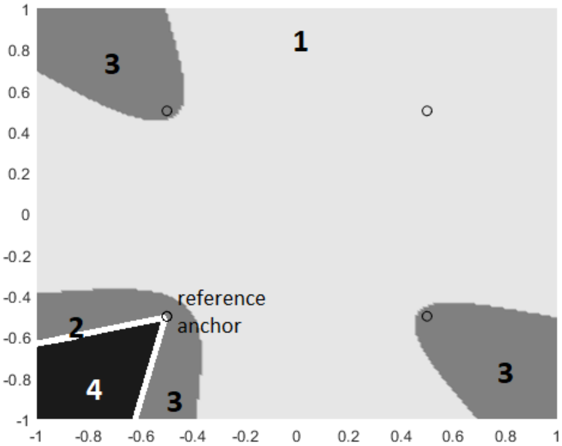

FIGURE 5. Example of the common conditions during the data processing for four anchors in corners of a square room.

3. $\alpha_{1,2}$ are real solutions and all $\hat{d}^{(3)} > 0$. The family line intersects only positive branch of the cone. Correct solution with shorter distance can be identified as one which minimizes the estimation error ε_2.
4. $\alpha_{1,2}$ are real solutions and $\hat{d}^{(3)} > 0$. The family line intersects only positive branch of the cone. Correct solution with longer distance can be identified as one which minimizes the estimation error ε_2.

In case of complex $\alpha_{1,2}$ the solution can be estimated as the cone point closest to the line (one unique solution). Updated parameter $\alpha_{1,2}$ then might be equal to

$$\alpha_{1,2} = -\frac{v_x\hat{x}^{(1)} + v_y\hat{y}^{(1)} - v_d\hat{d}^{(2)}}{v_x^2 + v_y^2 - v_d^2}, \tag{18}$$

where new distance $\hat{d}^{(2)} = \frac{-\hat{b} \pm \sqrt{\hat{b}^2 + 2\hat{a}\hat{c}}}{2\hat{a}}$ is a solution of quadratic equation:

$$\hat{a}\left(\hat{d}^{(2)}\right)^2 + \hat{b}\left(\hat{d}^{(2)}\right) + \hat{c} = 0, \tag{19}$$

where $\hat{a} = v_x^2 + v_y^2, \hat{b} = 2v_d\left(v_x\hat{x}^{(1)} + v_y\hat{y}^{(1)}\right)$ and $\hat{c} = v_d^2\left(\left(\hat{x}^{(1)}\right)^2 + \left(\hat{y}^{(1)}\right)^2\right) - \left(v_x\hat{y}^{(1)} - v_y\hat{x}^{(1)}\right)^2$. There are two possible locations of the line touching the cone: one appears for distance increasing and one for distance decreasing. Because of the fact we are searching solution for positive cone branch the larger distance should be chosen.

IV. P3WLS ALGORITHM PROPERTIES AND IMPROVEMENTS

To understand the P3WLS algorithm behavior in comparison to the 2WLS algorithm let's analyze location of anchors in the vertices of the 10 × 10 m square under 10 ps Gaussian measurement noise. For each point in the area we did 1000 measurements, and the 95% confidence interval $C_{0.95}$ was estimated for the distance to true location:

$$\Delta d = \sqrt{\left(\hat{x}^{(3)} - x\right)^2 - \left(\hat{y}^{(3)} - y\right)^2}, \tag{20}$$

$$P_{\Delta d}\left(\Delta d \leq C_{0.95}\right) = 0.95. \tag{21}$$

Near the major symmetry lines, we obtain the ill-condition problem which dramatically increases the error for the 2WLS algorithm (Fig. 6). Note, location estimation error is increased not only on the symmetry lines but also near them due to the noise which may cause ill-condition problem to appear there.

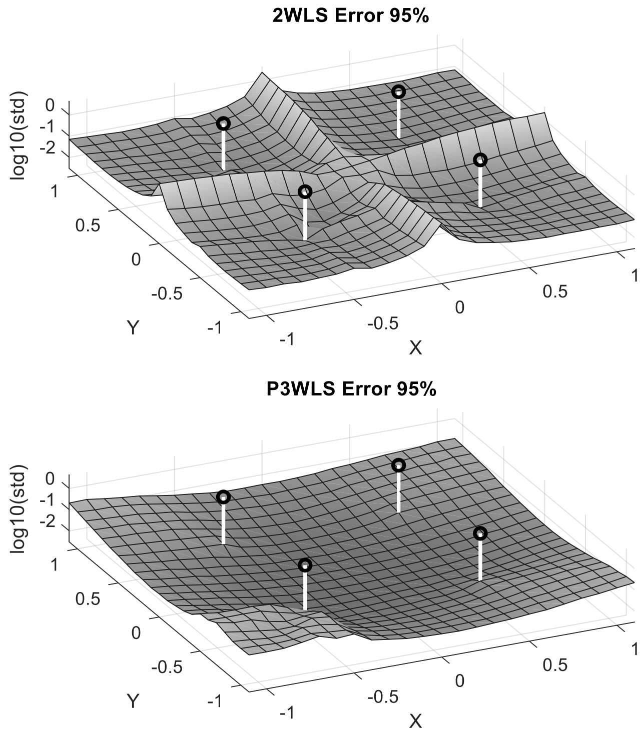

FIGURE 6. Example of error 95% confidence interval for the 100 ps Gaussian error for the 10 × 10 m 4 anchor's locations. The closest anchor (-0.5,-0.5) is chosen as the reference anchor.

In contrast, the P3WLS algorithm has no problems with the ill-conditioned system, because the solution family in this case is in the direction of the minimal eigenvalue eigenvector span and the algorithm error is minimal. But as soon as there is a strong relationship between tag coordinates and the distance to the reference, the system stiffness is minimal and solution family is not stretched along the minimal eigenvalue eigenvector span which leads to higher error in comparison to the 2WLS algorithm. Note, points where distance is more dependent on the coordinates are typically located outside the anchor's perimeter along conditions 2 and 4 (Fig. 5).

Summarizing the above, P3WLS has advantage in core area but has a minor disadvantage vs 2WLS outside the anchor's perimeter behind the closest anchor. Thus, solution clarification along the minimal eigenvalue eigenvector span should be done only in cases where is smaller relationship between independent parameter and coordinates. The obvious criteria for choosing the proper second and third steps is the matrix stiffness. In case the TDoA system stiffness is larger than a predefined threshold - choose estimation based on the family line evaluation, in other cases - use WLS method. An error plot example of a Hybrid Weighted Least Squares algorithm based on the stiffness criteria (HWLS(λ)) applied to the 10 × 10 m square anchor configuration under

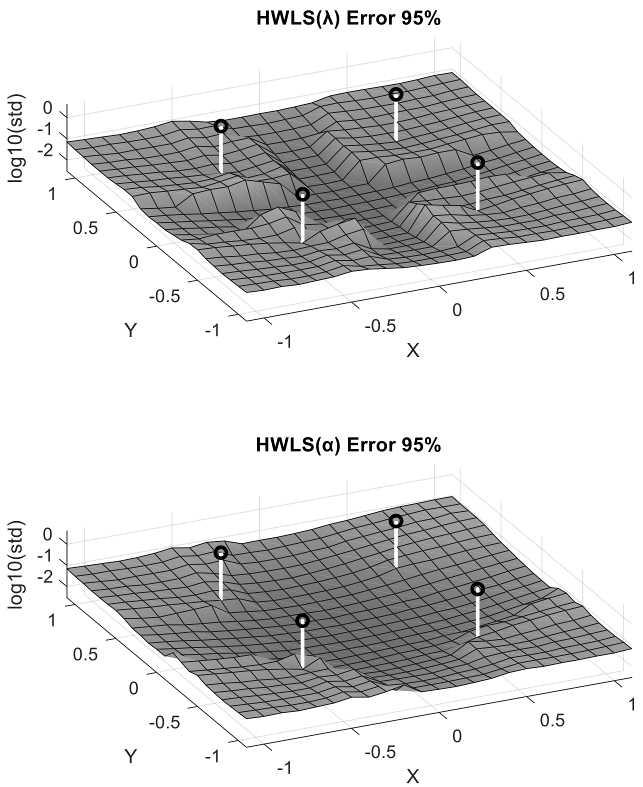

FIGURE 7. Example of error 95% confidence interval for the 100 ps Gaussian error for the 10 × 10 m 4 anchor's locations. The closest anchor (-0.5,-0.5) is chosen as the reference anchor.

10 ps Gaussian measurement noise is shown in Fig. 7. The algorithm properly switches to the family evaluation approach in case of the ill-condition problems on the symmetry lines and uses WLS in all other cases. Unfortunately, the stiffness criterion is not useful to choose an algorithm with smaller error in other points.

More appropriate criteria to recognize the poor relationship between the independent parameter and coordinates is the angle between family line and the XY plain. The larger the angle is the smaller the dependency on the XY coordinates. An error plot example of Hybrid Weighted Least Squares algorithm based on the angle criteria (HWLS(α)) applied to the 10 × 10 m square anchor configurations under a 10 ps Gaussian measurement noise is shown in Fig. 7. The criterion based on the angle behaves much better in choosing the optimal second and third algorithm stages and only struggles in area where both solutions provide comparable errors.

Special attention should be given to the reference anchor selection. More careful inspection of the Fig. 6 and Fig. 7 reveals the asymmetry in the error plots. In case the source is located closer to the reference anchor, the error increases. Looks like the optimal choice is the furthest anchor but this is not true in case of the strong noises when the furthest anchor may be the one with the largest noise. The optimal solution is to choose that reference anchor which provides the smallest error. One of the possible ways how to choose an optimal reference anchor is to use the angle between the family line and the XY plain as the criteria. The closer the angle is to the 45 degrees the larger the location error we expect to have. This is caused by the fact that solution the family intersection with the cone will have larger intersection ambiguity.

V. SIMULATION ENVIRONMENT DESCRIPTION

The P3WLS algorithm was tested in three environments with anchors located in the three different mesh patterns: square, hexagon, and triangular (Fig. 8). During a source motion the nearest anchors are selected for localization procedure. In case of the square pattern, there are two possible scenarios: if the source is in the middle of the mesh cell, the four nearest vertex/anchors are chosen forming a smaller square cell; if the source is next to a vertex, the five nearest anchors are selected which form larger square cell with the middle vertex in the center. Other cell configurations in the mesh pattern are not discussed because if signal can reach further anchors that means the solution is not optimized from cost perspective (number of anchors can be decreased). Smaller and larger square cells intersect each other and in case of a proper tracking algorithm the source is always located inside the core cell area (marked in grey). In case of a non-optimal tracking scenarios, the source may exit the core cell, and the whole cell should be analyzed. In case of a non-optimal tracking scenario, we estimate location errors up to the middle of the neighbor cells.

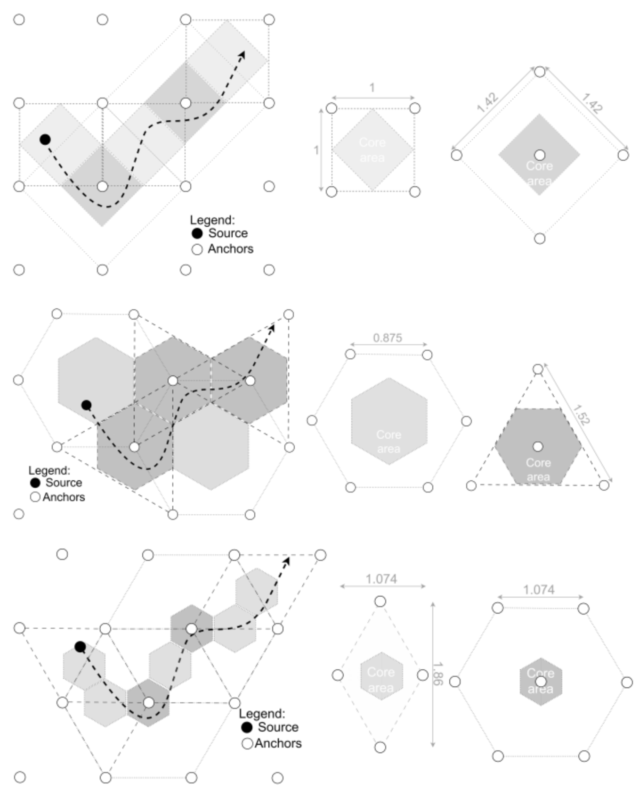

FIGURE 8. Three anchors location scenarios: a) square mesh pattern, b) hexagon mesh pattern, c) triangular mesh pattern.

In case of the hexagon mesh pattern there are also two possible scenarios: a hexagon cell if we are located closer

TABLE 1. 95% confidence interval localization error, m.

M	Cell	Gaussian Noise			Reference Desync			Non-Reference Desync			Shadowing		
		σ, ps	2WLS	P3WLS	τ, ps	2WLS	P3WLS	τ, ps	2WLS	P3WLS	Δ, m	2WLS	P3WLS
Square	Small square	10	9.07	0.01	10	8.01	0.00	10	8.44	0.00	0.5	85.82	0.36
		100	23.28	0.09	100	8.92	0.03	100	9.35	0.04	1	23.72	0.70
		1000	62.23	0.84	1000	64.11	0.29	1000	57.88	0.37	2	10.65	1.36
	Large square	10	0.01	0.01	10	0.00	0.00	10	0.00	0.00	0.5	0.34	0.46
		100	0.08	0.08	100	0.02	0.03	100	0.03	0.03	1	0.71	0.85
		1000	0.76	0.71	1000	0.21	0.32	1000	0.34	0.28	2	1.68	1.13
Hexagon	Hexagon	10	5.50	0.01	10	5.19	0.00	10	5.18	0.00	0.5	6.53	0.29
		100	5.52	0.07	100	5.52	0.03	100	5.52	0.03	1	7.66	0.57
		1000	7.06	0.71	1000	6.55	0.29	1000	6.60	0.26	2	8.53	1.11
	Trian-gular	10	0.11	0.01	10	0.01	0.00	10	0.09	0.00	0.5	1.50	0.45
		100	0.53	0.08	100	0.07	0.03	100	0.36	0.04	1	2.41	0.90
		1000	2.11	0.81	1000	0.37	0.36	1000	1.53	0.42	2	4.80	1.84
Triangular	Rhombus	10	0.15	0.01	10	0.06	0.00	10	0.10	0.00	0.5	1.71	0.42
		100	0.64	0.07	100	0.29	0.03	100	0.46	0.03	1	2.59	0.86
		1000	2.59	0.76	1000	1.11	0.28	1000	1.84	0.28	2	4.43	1.76
	Hexagon w middle node	10	0.02	0.01	10	0.01	0.00	10	0.01	0.00	0.5	0.66	0.34
		100	0.25	0.07	100	0.05	0.03	100	0.12	0.02	1	1.11	0.52
		1000	0.99	0.56	1000	0.39	0.31	1000	0.61	0.22	2	2.38	1.05

to the middle of the mesh cell, and a triangular cell in case the source is closer to the edge of the cell. In both scenarios the core region forms a hexagon area. The third anchor's pattern we analyze in the paper is the triangular mesh pattern. The two scenarios for this case: a rhomb cell in cases the source is between vertexes, and a hexagon cell with vertex in the middle in cases the source is next to any vertex. For the triangular pattern the core region also forms a hexagon region, but with much smaller area than in the case of the hexagon mesh pattern.

Note, length of the mesh pattern edges is chosen in such a way that results in an equal number of anchors per square area, to have similar solutions cost. Therefore, the hexagon mesh pattern has smaller edge length than the square mesh pattern (0.875x), and a triangular mesh pattern edge is larger than the square mesh pattern edge in 1.074x.

VI. SIMULATION NOISE/MEASUREMENT ERROR MODELS

There are several different perturbation scenarios that can occur in real-life applications: Gaussian noise, anchors desynchronization and shadowing.

The most common measurement error in the TDoA systems is the Gaussian white noise, which is usually created by the thermal electronic noise and/or by interference with external radio signals. In ideal case scenarios i_{th} receiver capture the exact moment of signal arrival t_i. Subsequently, TDoA is calculated relative to a j_{th} reference receiver ToA: $\tau_{ij} = t_i - t_j$. However, in real-world scenarios, achieving distortion-free signal measurements is unattainable thus in our simulations we introduce time jitters Δt_{i}, Δt_j added to each time of arrival t_i and t_j correspondingly: $\Delta t_{\text{i}} = N\left(0, \sigma^2\right)$, $\Delta t_j = N\left(0, \sigma^2\right)$, where σ is 0.01, 0.1, or 1 ns.

TDoA system requires high-accuracy time synchronization between all anchors and even small synchronization mistakes can cause large localization error. Receiver desynchronization appears in a TDoA system as a systematic error effecting time of arrival and usually depends on the time since the last anchor nodes synch. Desynchronization can be observed in non-reference & reference anchors with different effect on the TDoA system operation. Non-reference anchors desynchronization has only impact on its own TDoA and can be described by time of arrival offset uniform distribution: $\Delta t_{\text{i}} = U(-\tau, \tau)$, where τ is a maximal possible desynchronization (0.01, 0.1, or 1 ns in our experiments). Reference receiver desynchronization has impact on all TDoA measurements and can be described by time of arrival offset uniform distribution: $\Delta t_j = U(-\tau, \tau)$.

A TDoA system in a complex environment suffers from a multipath propagation and LoS shadowing. In such case the system may report a reflected (longer) path time delay instead of the true one. In the paper we evaluate the shadowing effect on the one of the anchors and describe this phenomenon by time of arrival offset uniform distribution: $\Delta t_j = U(0, \Delta/c)$, where c is the speed of light, and Δ is maximal possible distance offset (0.5, 1, or 2 m).

VII. PERFORMANCE OF THE P3WLS METHOD

Table 1 contains 95% confidence interval of the error for 2WLS and P3WLS algorithms in case of Gaussian Noise perturbations, reference and non-reference desynchronization and a shadowing for different mesh-cell scenarios. Small square cell dimension in this case was selected to be 10m and all other cells sizes were selected in a way to keep the solutions cost identical. Obviously the 2WLS algorithm shows the worst performance because of the ill-condition problem in case of small square and hexagon cells where error is extremely large and commensurate with the cell size. In case of the triangular and rhombus cells, the estimated localization error was quite large, although the ill condition problem is not expected to appear in the core region of the cells, but strong perturbations distort the matrix so significantly, so the ill-condition problem sometimes is observed even in the core region.

The P3WLS algorithm shows a significant advantage vs 2WLS algorithm for all cells except the large square cell and hexagon with core node were both algorithms shows comparable results. In general, the P3WLS algorithm shows ∼1 cm error for 10 ps Gaussian noise floor, ∼10 cm error for 100 ps noise and ∼1 m for 1 ns. Reference and non-reference desynchronization perturbations are less affecting the TDoA system. Expected error is less than 0.3 cm for 10 ps desync, ∼3 cm for 100 ps, and ∼30 cm for 1 ns. Note, the reference synchronization affects only one reference anchor but is as serious as effect of all non-reference synchronization anchors. Accordingly, the common mode perturbations are as dangerous as the random one. The worst location errors we obtain in case of shadowing perturbations. Shadowing offset of 0.5 m results in ∼ 40 cm error, 1 m offset - in ∼80 cm, and 2 m offset results in 1-2 m error.

An optimal mesh configuration for the 2WLS algorithm is triangular with expected error 2 m in LoS scenarios and ∼4 m in nLoS scenarios. Hexagonal and square mesh patterns are not recommended due to the ill-condition problem. Whereas P3WLS algorithm can operate in any mesh environment resulting in <1 m error for LoS and <2 m for nLoS for core regions of the cells which implies optimal neighbor anchors scenario.

In case of proper cell is difficult to localize due to the strong nLoS environment or source tracking is not possible, we may expect a wrong cell is selected and the area outside the core region is analyzed. In such case the P3WLS algorithm may operate in third and fourth conditions (Fig. 5) where hybrid algorithms are recommended.

To analyze the behavior outside the core cell region the root mean square (RMS) error was calculated for 2WLS, P3WLS and for hybrid algorithms in different mesh scenarios with Gaussian noise (Fig. 9-11). The hybrid HWLS(λ) and HWLS(α) algorithms use eigenvalues and angle criteria to switch to a proper algorithm, and the decisions are made based on the criteria value comparison with predefined thresholds. The thresholds are optimized for each cell separately to obtain a best performance. Simulations within the core region are referred as an optimal switching scenario which implies the proper cell is chosen all the time the source moves outside the previous core cell area. A non-optimal switching scenario implies situations when the source tracking faces some issues and incorrect anchors are used from the neighbor cells.

Because the ill-condition problem mainly appears in the core region, the 2WLS algorithm results in the smaller error for the non-optimal switching due to the smaller ill-condition problem probability in the larger region. Such behavior is typical for the square and the hexagon mesh patterns, but in case of the triangular mesh pattern, an optimal switching scenario has a huge advantage vs non-optimal one because of the ill-condition region lies outside the core region.

There is no advantage in usage the hybrid algorithms for the optimal switching scenarios as the P3WLS algorithm has no issue in the core cell area. That's exactly why the

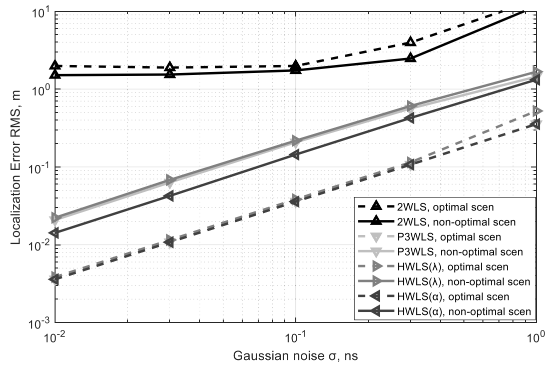

FIGURE 9. Algorithms localization error for square mesh pattern.

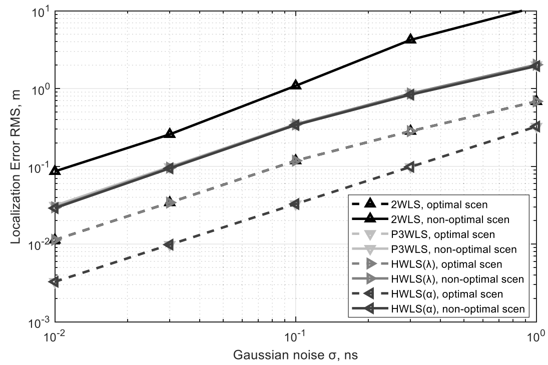

FIGURE 10. Algorithms localization error for triangular mesh pattern.

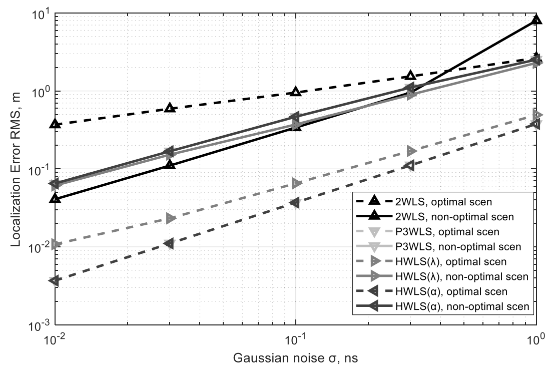

FIGURE 11. Algorithms localization error for hexagon mesh pattern.

HWLS(α) algorithm performance fully coincide with the P3WLS one for the optimal switching scenario. However, in case of non-optimal switching scenario the HWLS(α) algorithm provides up to 25% smaller error for a square mesh pattern by switching to 2WLS algorithm outside the cell. Unfortunately for the triangular and hexagon mesh patterns the advantage is minimal. In contrast, the HWLS(λ) algorithm shows the best performance for the hexagon mesh but is slightly worse for the square mesh pattern.

Table 2 summarizes the simulation results and reports the ratio of averaged noise floor across all simulation vs the best possible result achievable for the P3WLS (and HWLS(α)) algorithm and the triangular mesh pattern. The 2WLS algorithm can be used in case of the triangular pattern

TABLE 2. Algorithms comparison for different conditions, error ratio, times.

Algo	Scen.	Square	Triangular	Hexagon
2WLS	Opt.	186.7	3.1	44.7
	Non-opt.	145.0	32.6	13.8
P3WLS	Opt.	1.1	1.0	1.1
	Non-opt.	5.8	9.0	14.0
HWLS(λ)	Opt.	1.3	3.1	2.2
	Non-opt.	6.3	8.8	12.3
HWLS(α)	Opt.	1.1	1.0	1.1
	Non-opt.	4.3	8.6	14.0

and the optimal switching scenario only with a 3x larger error in comparison to the P3WLS algorithm which can be used with any mesh pattern. The HWLS(λ) algorithm is recommended only for the square mesh pattern with the optimal switching scenario. In case of the non-optimal switching scenario, the HWLS(α) algorithm in the square mesh pattern is recommended with the 4.3x error increase vs the optimal switching scenario.

There is no preferable mesh pattern as soon as the proper algorithm is used for the optimal switching scenarios. Expected error differences are less than 10%. But if the optimal source tracking cannot be guaranteed and we may select incorrect anchors for TDoA measurements, the square pattern with the HWLS(α) algorithm is preferable. The error increase is expected to be close to 4x in this case.

VIII. CONCLUSION

Time difference of arrival is a very popular and efficient technique for devices localization when a network of synchronized anchors is available. Such a technology is strongly demanded by the warehouse/manufacturer businesses for asset tracking because it can easily work with thousands of tags covering large areas, with minimal requirements to tags power sources that work by simple power-efficient broadcasting of small-period location messages. The cost of such TDoA systems is mostly defined by the number of anchors in the mesh, therefore a requirement to lower the solutions cost demands understanding of optimal mesh configuration and performance that can be reached. Unfortunately decreasing the number of anchors in such systems leads to regular mesh pattern cells formation with symmetry susceptible to the ill-condition problems for the classical low complexity 2WLS algorithms. The paper proposes a new set of algorithms developed to solve the ill-condition problem without switching to more computationally complex approaches. The developed P3WLS algorithm utilizes a family of solutions that are formulated during an additional step in the solution flow analyzing relations between an independent variable introduced in the 2WLS approach and source coordinates. The P3WLS algorithm fully solves the problem for the core region of the anchor mesh cells. Unfortunately, the P3WLS algorithm has its own weaknesses and outside the anchor's cell sometimes results in slightly worse results. To deal with the problems outside the cells, two hybrid algorithms were developed which switch between several methods based on the proposed eigenvalue ratio and independent parameter correlation criteria.

The verification of the proposed methods was done by simulation TDoA localization system for various anchor mesh patterns under different perturbations such as Gaussian noise to emulate thermal noise and external noise interference, reference and non-reference anchor desynchronization, and node shadowing. The P3WLS algorithm shows significant advantage vs 2WLS for all cases, including multipath conditions with a shadowing.

One of the experiments considers situations where the system uses a non-optimal set of anchors (not closest ones) to determine a tag position. It happens in case of multipaths, shadowing, noise influence or synchronization problems. It is possible in this cases that a tag appears outside of anchors perimeter that noticeably decreases accuracy of tag location determination. The results of simulations give understanding of optimal mesh configuration for different mesh patterns and switching scenarios. For an optimal switching scenario all mesh patterns with the same number of nodes per square shows similar results for the best P3WLS and HWLS(α) algorithms. In case of the non-optimal scenario, when the source may appear outside the cell, the square mesh pattern shows the best performance with the 4.3x degradation in comparison to the optimal scenario.

In the following work we plan to accomplish additional simulation and provide complete comparison with other algorithms for TDoA location determination, especially the NN-based, deeper analyze a question of an optimal selection of the best anchor nodes set and reference node selection criteria, advantages of tracking capabilities and UWB channel impulse response data usage for better accuracy in case of large number anchor nodes mesh networks.

REFERENCES

[1] J. Ni, D. Arndt, P. Ngo, C. Phan, K. Dekome, and J. Dusl, "Ultra-wideband time-difference-of-arrival high resolution 3D proximity tracking system," in *Proc. IEEE/ION Position, Location Navigat. Symp.*, Location and Navigation Symposium, India, May 2010, pp. 37–43, doi: 10.1109/PLANS.2010.5507198.

[2] M. Luo, X. Chen, S. Cao, and X. Zhang, "Two new shrinking-circle methods for source localization based on TDoA measurements," *Sensors*, vol. 18, no. 4, p. 1274, Apr. 2018, doi: 10.3390/S18041274.

[3] L. Lin, H. C. So, F. K. W. Chan, Y. T. Chan, and K. C. Ho, "A new constrained weighted least squares algorithm for TDOA-based localization," *Signal Process.*, vol. 93, no. 11, pp. 2872–2878, Nov. 2013, doi: 10.1016/J.SIGPRO.2013.04.004.

[4] G. Lindfield and J. Penny, *Chapter 5—Solution of Differential Equations*, 4th ed., New York, NY, USA: Academic, 2019, ch. 5, pp. 239–299, doi: 10.1016/B978-0-12-812256-3.00014-2.

[5] S. M. Sheikh, H. M. Asif, K. Raahemifar, and F. Al-Turjman, "Time difference of arrival based indoor positioning system using visible light communication," *IEEE Access*, vol. 9, pp. 52113–52124, 2021, doi: 10.1109/ACCESS.2021.3069793.

[6] Y. T. Chan and K. C. Ho, ''A simple and efficient estimator for hyperbolic location,'' *IEEE Trans. Signal Process.*, vol. 42, no. 8, pp. 1905–1915, Aug. 1994, doi: 10.1109/78.301830.

[7] C. Mensing and S. Plass, ''Positioning algorithms for cellular networks using TDOA,'' in *IEEE Int. Conf. Acoust. Speed Signal Process. Proc.*, vol. 4, Jun. 2006, pp. 1–24, doi: 10.1109/ICASSP.2006.1661018.

[8] J. Smith and J. Abel, ''Closed-form least-squares source location estimation from range-difference measurements,'' *IEEE Trans. Acoust., Speech, Signal Process.*, vols. ASSP-35, no. 12, pp. 1661–1669, Dec. 1987, doi: 10.1109/TASSP.1987.1165089.

[9] D. Torrieri, ''Statistical theory of passive location systems,'' *IEEE Trans. Aerosp. Electron. Syst.*, vols. AES-20, no. 2, pp. 183–198, Mar. 1984, doi: 10.1109/TAES.1984.310439.

[10] K. Cheung, H. So, W.-K. Ma, and Y. Chan, ''A constrained least squares approach to mobile positioning: Algorithms and optimality,'' *EURASIP J. Adv. Signal Process.*, vol. 2006, no. 1, Dec. 2006, Art. no. 020858, doi: 10.1155/ASP/2006/20858.

[11] J. Pan, ''Multi-station TDOA localization method based on Tikhonov regularization,'' in *Proc. 7th Int. Conf. Intell. Comput. Signal Process. (ICSP)*, Apr. 2022, pp. 1903–1906, doi: 10.1109/ICSP54964.2022.9778449.

[12] Z. Wang, D. Hu, Y. Zhao, Z. Hu, and Z. Liu, ''Real-time passive localization of TDOA via neural networks,'' *IEEE Commun. Lett.*, vol. 25, no. 10, pp. 3320–3324, Oct. 2021, doi: 10.1109/LCOMM.2021.3097065.

[13] S. Pak, B. K. Chalise, and B. Himed, ''Target localization in multistatic passive radar systems with artificial neural networks,'' in *Proc. Int. Radar Conf. (RADAR)*, Toulon, France, Sep. 2019, pp. 1–5, doi: 10.1109/RADAR41533.2019.171252.

[14] A. Kirmaz, T. Sahin, D. S. Michalopoulos, and W. Gerstacker, ''ToA and TDoA estimation using artificial neural networks for high-accuracy ranging,'' *IEEE J. Sel. Areas Commun.*, vol. 41, no. 12, pp. 3816–3830, Dec. 2023, doi: 10.1109/JSAC.2023.3322803.

[15] A. Niitsoo, T. Edelhäußer, and C. Mutschler, ''Convolutional neural networks for position estimation in TDoA-based locating systems,'' in *Proc. Int. Conf. Indoor Positioning Indoor Navigat. (IPIN)*, Nantes, France, Sep. 2018, pp. 1–8, doi: 10.1109/IPIN.2018.8533766.

[16] S. Bhattacharya and J. Choi, ''RNN-based robust smartphone indoor localization on ultra-wideband DL-TDOA,'' in *Proc. IEEE Int. Conf. Commun. Workshops (ICC Workshops)*, Rome, Rome, Italy, May 2023, pp. 500–505, doi: 10.1109/ICCWORKSHOPS57953.2023.10283529.

[17] Y. Chen, T. Xiang, X. Chen, and X. Zhang, ''Map-assisted TDOA localization enhancement based on CNN,'' 2023, *arXiv:2311.01291*.

[18] N. Marchand, ''Error distributions of best estimate of position from multiple time difference hyperbolic networks,'' *IEEE Trans. Aerosp. Navigational Electron.*, vols. ANE-11, no. 2, pp. 96–100, Jun. 1964, doi: 10.1109/TANE.1964.4502170.

[19] C. Yanli, H. Yuyao, and F. Yao, ''Multiple circle linkage's search target localization of the vibration source algorithm,'' *Optik*, vol. 131, pp. 207–214, Feb. 2017, doi: 10.1016/J.IJLEO.2016.11.094.

[20] J. N. Moutinho, R. E. Araujo, and D. Freitas, ''Indoor localization with audible sound—Towards practical implementation,'' *Pervas. Mobile Comput.*, vol. 29, pp. 1–16, Jul. 2016, doi: 10.1016/J.PMCJ.2015.10.016.

[21] R. Zekavat and R. M. Buehrer, *Handbook of Position Location: Theory, Practice and Advances*, vol. 27. Hoboken, NJ, USA: Wiley, 2011, doi: 10.1002/9781118104750.

[22] D. Coppens, A. Shahid, S. Lemey, B. Van Herbruggen, C. Marshall, and E. De Poorter, ''An overview of UWB standards and organizations (IEEE 802.15.4, FiRa, Apple): Interoperability aspects and future research directions,'' *IEEE Access*, vol. 10, pp. 70219–70241, 2022, doi: 10.1109/ACCESS.2022.3187410.

[23] *Channel Sounding CR_PR, Bluetooth SIG Specification Draft*. Accessed: May 17, 2024. [Online]. Available: https://www.bluetooth.com/specifications/

[24] (2024). *Texas Instruments BLE CS Application Note: High Accuracy, Low Cost, Secure Ranging With Bluetooth Channel Sounding*. Accessed: May 17, 2024. [Online]. Available: https://www.ti.com/lit/an/swra791/swra791.pdf?ts=1716004295036

[25] T. Roth, F. Freyer, M. Hollick, and J. Classen, ''AirTag of the clones: Shenanigans with liberated item finders,'' in *Proc. IEEE Secur. Privacy Workshops (SPW)*, San Francisco, CA, USA, May 2022, pp. 301–311, doi: 10.1109/SPW54247.2022.9833881.

[26] J. D. Lambert, *Numerical Methods for Ordinary Differential Systems*. Hoboken, NJ, USA: Wiley, 1992.

[27] I. Javorskyj, D. Dehay, and I. Kravets, ''Component statistical analysis of second order hidden periodicities,'' *Digit. Signal Process.*, vol. 26, pp. 50–70, Mar. 2014, doi: 10.1016/J.DSP.2013.12.002.

[28] Y. Zou, H. Liu, and Q. Wan, ''An iterative method for moving target localization using TDOA and FDOA measurements,'' *IEEE Access*, vol. 6, pp. 2746–2754, 2018.

IGOR KRAVETS received the master's degree of science in radio physics and electronics from Ivan Franko National University of Lviv, in 2003, and the Ph.D. degree in mathematics modeling and numerical methods from Lviv Polytechnic National University, Lviv, Ukraine, in 2007. He has been an Associate Professor of condition monitoring of materials and structures with Karpenko Physico-Mechanical Institute, since 2012. He has been a Senior Associate Professor and a Senior Researcher with Karpenko Physico-Mechanical Institute, since 2017. He has been a Senior Principal Engineer of applied systems research group with Infineon Technologies AG, since 2012. Merit Order for Young Scientists by the National Academy of Sciences of Ukraine.

OLEG KAPSHII received the Ph.D. degree in mathematics modeling and numerical methods from Lviv Polytechnic National University, Lviv, Ukraine, in 2006.

From 2000 to 2020, he was a Researcher with Karpenko Physico-Mechanical Institute of the NAS, Ukraine. Since 2014, he has been a Senior Principal Engineer of applied systems research group with Infineon Technologies AG. His research interests include signal processing, wireless communication, embedded systems, and machine learning.

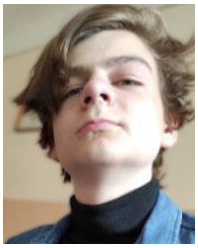

OSTAP SHUPARSKYY is currently pursuing the bachelor's degree in micro- and nano-systems with Ivan Franko National University of Lviv. His research interests include signal processing, embedded systems, wireless communication, and machine learning.

ANDRIY LUCHECHKO received the master's degree in physics, in 2002, and the Ph.D. and D.Sc. degrees in physical and mathematic sciences from Ivan Franko National University of Lviv, Ukraine, in 2007 and 2020, respectively. He is currently a Professor with the Department of Sensor and Semiconductor Electronics, Ivan Franko National University of Lviv. He has co-authored more than 150 research articles among them, about 100 are cited in Scopus. He took part in many national research projects and international grants. His research and teaching interests include sensors, the Internet of Things, embedded systems, TSL and OSL dosimetry, and materials for electronic technics and phosphors. He was a recipient of the Cabinet of Ministers of Ukraine Fellowship from the Ministry of Education for Young Scientists, received the honorary diplomas of Rector of Lviv University, and Department of Education and Science of the Lviv Regional State Administration.